Atmospheric
Chemistry
and Physics

Research article

Formation of highly absorptive secondary brown carbon through nighttime multiphase chemistry of biomass burning emissions

Ye Kuang[1,2], **Biao Luo**[1,2], **Shan Huang**[1,2], **Junwen Liu**[1,2], **Weiwei Hu**[3], **Yuwen Peng**[1,2], **Duohong Chen**[4], **Dingli Yue**[4], **Wanyun Xu**[5], **Bin Yuan**[1,2], and **Min Shao**[1,2]

[1]Institute for Environmental and Climate Research, College of Environment and Climate,
Jinan University, Guangzhou 511443, China
[2]Guangdong-Hongkong-Macau Joint Laboratory of Collaborative Innovation for Environmental Quality,
Guangzhou 511443, China
[3]State Key Laboratory of Organic Geochemistry and Guangdong Key Laboratory of Environmental Protection
and Resources Utilization, Guangzhou Institute of Geochemistry, Chinese Academy of Sciences,
Guangzhou 510640, China
[4]Guangdong Ecological and Environmental Monitoring Center, State Environmental Protection Key Laboratory
of Regional Air Quality Monitoring, Guangzhou 510308, China
[5]State Key Laboratory of Severe Weather, Key Laboratory of Atmospheric Chemistry, Institute of Atmospheric
Composition, Chinese Academy of Meteorological Sciences, Beijing 100081, China

Correspondence: Ye Kuang (kuangye@jnu.edu.cn) and Shan Huang (shanhuang_eci@jnu.edu.cn)

Abstract. Biomass burning is a major global source of both primary brown carbon (BrC) and reactive trace gases in the atmosphere and thus has a significant impact on global climate and regional atmospheric chemistry. However, a substantial gap remains in our understanding of the nighttime evolution of biomass burning emissions. Here we present prominent nighttime formation of secondary organic aerosol (Night-OA) with strong absorptivity but markedly different spectral dependence from that of primary biomass burning organic aerosols, which was observed during autumn in the Pearl River Delta region of China when biomass burning plumes prevailed. Our results demonstrate that the formation of Night-OA appeared to have high dependence on both the magnitudes of biomass burning emissions at nightfall and available oxidants of NO_2 and O_3. Active nighttime NO_3 radical chemistry was characterized by quick O_3 depletion and almost zero concentration of NO. The rapid decrease in NO_2 coincident with the quick nitrate formation suggests that the rapid NO_2 consumption supplied the NO_3 and N_2O_5 reaction chains. However, the quickest Night-OA formation occurred when nitrate formation ceased and relative humidity reached maximum, and it mainly added mass to aerosol water-abundant diameter ranges. This co-variation suggests that gas-phase reactions of biomass burning precursors, along with aqueous-phase chemistry involving preexisting hygroscopic aerosols in the diluted plume, likely work in concert to promote the rapid nighttime formation of Night-OA. Preexisting background aerosols are generally much more hygroscopic than the aerosols directly emitted from biomass burning. Incorporating the important role of background aerosols in the aging of diluted biomass burning plumes would be valuable in future laboratory and model simulation studies. The proposed mechanisms for secondary BrC formation have broad implications for the climate and air quality impacts of biomass burning, including the interaction between biomass burning plumes and background aerosols in humid regions, as well as with water-abundant pyroconvection clouds.

1 Introduction

Light-absorbing organic aerosols, termed brown carbon (BrC) (Andreae and Gelencsér, 2006), absorb solar radiation and warm the atmosphere, act as potential photosensitizers, and alter atmospheric oxidation capacity (Liu et al., 2020), thus having a profound impact on atmospheric chemistry, air quality, and climate (Jo et al., 2016). Biomass burning activities happen frequently across the globe due to natural and anthropogenic activities injecting large amounts of fine organic aerosols (known as biomass burning organic aerosol, BBOA) and trace gases into the global atmosphere, thereby acting as a major global source of primary aerosols and volatile organic compounds (Andreae and Merlet, 2001; Akagi et al., 2011; Andreae, 2019; van der Werf et al., 2017) and thus having a significant impact on global climate (Liu et al., 2021; Yu et al., 2019, 2021). The freshly emitted BBOA is highly absorptive near ultraviolet wavelengths and considered a major contributor to atmospheric BrC (Wang et al., 2016). A number of laboratory studies revealed that secondary organic aerosol (SOA) formed from the oxidation of biomass burning precursors (BBSOAs) is also absorptive (Saleh et al., 2013). However, the importance of secondary BrC formed from biomass burning precursors remains uncertain.

Both daytime and nighttime chemistries play a significant role in aging biomass burning plumes and associated secondary SOA and BrC formation. Daytime aging of biomass burning emissions and its impacts on SOA formations have previously been extensively investigated (Hodshire et al., 2019). Those investigations found that the formed SOA contributed substantially to BrC (Kumar et al., 2018; Saleh, 2020), which was confirmed by field measurements. For example, Palm et al. (2020) observed that daytime oxidation of emitted phenolic compounds contributed substantially to BBSOA formation from direct gas emissions, with products being highly absorptive. Compared with daytime aging experiments of biomass burning emissions, laboratory studies representative of night chemistry are scarce. At night, the consumptions of O_3 and OH is much faster than their formation rates due to the absence of photochemical reactions; thus the atmospheric concentration of these two oxidants reduce rapidly after sunset. The depletion of O_3 through NO_2 oxidation generates NO_3 radicals that act as a major oxidant during nighttime periods and drive the tropospheric nighttime chemistry (Wang et al., 2023a). Decker et al. (2019) investigated the nighttime chemical transformation in biomass burning plumes using a box model, which was initialized by aircraft observations, with results demonstrating NO_3 radical loss mostly due to reactions with biomass burning volatile organic compounds (VOCs). In recent years, a number of laboratory studies using NO_3 as the oxidant were carried out to explore the influences of nighttime aging on SOA formation from biomass burning and associated BrC evolutions (Cheng et al., 2020; Li et al., 2020a; Jiang et al., 2019; Tiitta et al., 2016; Hartikainen et al., 2018). Their results demon-

strated that both the nighttime aging of BBOA aerosols and biomass burning VOC precursors such as pyrrole can potentially act as important sources of SOA and BrC. However, contributions derived from laboratory studies cannot be directly linked with SOA and BrC contribution magnitudes within ambient nighttime atmosphere. Kodros et al. (2020) further highlighted the importance of nighttime processing of biomass burning emissions as an important global source of SOA based on combined results from laboratory and field observations.

Nevertheless, field measurements that observe nighttime evolutions of biomass burning plumes and directly confirmed significant contributions of SOA and BrC from nighttime aging of biomass burning emissions are largely lacking. Only one field measurement study has observed a substantial increase in BrC light absorption during a night-long biomass burning event and identified nitroaromatics in abundance within aged BBOA aerosols, contributing greatly to light absorption (Lin et al., 2017; Bluvshtein et al., 2017). Based on this study, it was hypothesized that nighttime chemistry involving NO_3 radical oxidation of primary BBOA might play a significant role in BrC transformation. Nighttime conditions are typically characterized by high atmospheric relative humidity (RH) caused by temperature decreases, therefore likely resulting in abundant aerosol water which might favor aqueous SOA and BrC formation (Wang et al., 2019b). However, most previous laboratory studies have not investigated the role of RH or multiphase chemistry in the nighttime aging of biomass burning plumes. Kodros et al. (2022) found that the nighttime oxidation of biomass burning emissions was sensitive to RH; however, they could not conclude what role RH played. Their results demonstrated that the homogenous gas-phase oxidation and the subsequent condensation of lower-volatility vapors were probably the dominant process. However, they could not rule out the possible role of heterogeneous oxidation processes. In addition, biomass burning emissions were injected into the air where abundant aerosols (including organics and inorganics) already exist whose overall water uptake abilities are likely much higher than primary biomass burning aerosols, which is closer to being hydrophobic under subsaturated conditions (Tao et al., 2024). However, roles of existing background aerosols in aging of biomass burning plumes were rarely investigated. Therefore, how nighttime NO_3 radical chemistry coordinates with heterogeneous multiphase reactions under high-RH conditions to affect SOA and BrC formations remains unexplored. Adding to this knowledge gap is how biomass burning emissions contribute to SOA and secondary BrC formation.

In this study, we report substantial amounts of highly absorptive SOA likely formed during nighttime mainly from biomass burning emissions. The potential formation mechanisms of nighttime SOA formation are investigated based on real-time measurements of parameters such as gaseous pollutants, aerosol physical and chemical properties, and meteorological factors. Our results revealed that coordinated

nighttime multiphase chemistry of biomass burning emissions likely formed highly absorptive SOA, which improved our current understanding of the nighttime aging of biomass burning emissions and might also have significant implications for cloud processing of biomass burning. Additionally, this study is a companion paper to Luo et al. (2022), where we proposed an improved absorption Ångström exponent (AAE) ratio method for deriving multiwavelength BrC absorptions from multiwavelength aerosol absorption measurements using an Aethalometer and investigated comprehensively the size distribution, absorption and scattering, and the refractive index of primary BBOA.

2 Materials and methods

2.1 Field measurements

A field campaign was conducted from 30 September to 17 November 2019 at a regional background site of the Pearl River Delta. This site is located in the countryside of Heshan county, about 55 km away from the megacity of Guangzhou and on the top of hill whose surroundings are small villages and residential towns. Routine observations of air pollutants such as carbon monoxide, ozone, nitrogen dioxides, and $PM_{2.5}$ (particulate matter with aerodynamic diameter less than 2.5 μm) and meteorological parameters such as RH, temperature, and wind speeds and directions (model WXT520, Vaisala, Finland) were managed by the provincial environmental monitoring authority, and this site is authorized as a regional background supersite. During the observation period, intensive aerosol measurements including aerosol optical properties, aerosol size distributions, and aerosol chemical compositions were also performed to investigate relationships between aerosol physical properties and aerosol chemical compositions. The aerosol scattering properties and aerosol hygroscopicity were measured using a humidified nephelometer (Aurora 3000) system (Kuang et al., 2021). Aerosol absorptions of multiple wavelengths were measured using an Aethalometer (AE33; Magee AE33; Drinovec et al., 2015). Aerosol size distributions were measured jointly by using a scanning mobility particle sizer (SMPS; TSI 3080) and an aerodynamic particle sizer (APS; TSI Inc., model 3321). For more details on the site and setup of instruments, please refer to Kuang et al. (2021) and Luo et al. (2022).

The submicron aerosol chemical compositions were measured using a soot particle high-resolution time-of-flight aerosol mass spectrometer (SP-AMS; Aerodyne Research, Inc., Billerica, MA, USA). The setup and validation of SP-AMS measurements were performed and discussed in Kuang et al. (2021) and thus are not detailed here. Source identification of organic aerosols was performed using the commonly used positive matrix factorization (PMF). Two primary OA factors and four secondary OA factors are identified, and the determination of

PMF factors are thoroughly discussed in Luo et al. (2022). The two primary OA factors include biomass burning organic aerosols (BBOAs) and hydrocarbon-like organic aerosols (HOAs). The biomass burning emissions represent the most important primary sources during the observations as discussed in Luo et al. (2022), and its most prominent activities were usually observed near sunset (Fig. 1a). The four SOA factors include more-oxygenated organic aerosols (MOOAs, O/C = 1), less-oxygenated organic aerosols (LOOAs, O/C = 0.72), nighttime-formed organic aerosols (Night-OAs, O/C = 0.32), and aged BBOAs (aBBOAs, O/C = 0.39), named in previous work (Kuang et al., 2021; Luo et al., 2022; Wu et al., 2024). The Night-OA factor was characterized by its obvious correlation with nitrate, and they both exhibited an obvious increase after sunset (Fig. S1). The name of aBBOA was originally because of its correlation with $C_6H_2NO_4^+$, which is a typical fragment of the aged BBOA component nitrocatechol (Bertrand et al., 2018). However, this factor was renamed BB-SOA as discussed in the following paragraph. The mass spectral profiles, time series of these organic aerosol factors, and details about the determination of these factors are introduced in the supplement of Luo et al. (2022). Note that the AE33 measurements were only available until 1 November, while SP-AMS measurements were available until 18 November, resulting in different time frames of different time series.

Given that PMF analysis is fundamental to our study, the mass spectral profiles of factors are provided in Fig. S1, and key aspects of the resolved results are explained here, particularly concerning the naming of aBBOA. In previous studies (Kuang et al., 2021; Luo et al., 2022), we already realized that the correlation between aBBOA and $C_6H_2NO_4^+$ was actually weak ($R = 0.31$), suggesting that it might not fully be constituted of aging products of primary BBOA considering its O/C was even lower than that of BBOA. The following clues demonstrate that aBBOA is mostly secondary and formed from the gas-phase reactions: (1) aBBOA exhibited similar diurnal behavior to LOOA, showing clear daytime photochemical production (Fig. S1), and (2) the increase in aBBOA loading enhances organic aerosol hygroscopicity despite its low O/C ratio, as demonstrated by Kuang et al. (2021). In contrast, primary organic aerosols have not been observed to enhance overall organic aerosol hygroscopicity (Kuang et al., 2020b, 2024; Tao et al., 2024). (3) aBBOA primarily added mass to the condensation mode diameter range (see discussions on OA factor size distributions in the supplement of Luo et al., 2022), suggesting that aBBOA forms from vapor condensation after gas-phase reactions (Kuang et al., 2020a). Furthermore, the following facts indicate that aBBOA is formed from gas-phase reactions of biomass burning precursors. (1) An evening peak in aBBOA around 19:00 LT (local time) occurs just after the peak of BBOA emissions, as shown in Fig. S1, although a small portion of aBBOA may be directly emitted (the increase in aBBOA during BBOA emissions accounts for an average of 8 %

of the mass increase in biomass burning events; Fig. 3 of Luo et al., 2022). (2) The daytime formation of aBBOA is correlated with the biomass burning intensity from the previous night (Wu et al., 2024). (3) The high absorptivity of aBBOA (introduced in Sect. 3.1) is comparable to SOA formed from biomass burning precursors (Saleh et al., 2013). As demonstrated in previous indoor experiments on biomass burning emissions (Yee et al., 2013; Ahern et al., 2019), SOA formation from gas-phase reactions could have a low O/C during short oxidation periods, which helps explain the low O/C of aBBOA. Given these convincing arguments, the original designation of aBBOA may not be appropriate. Therefore, we have renamed this factor BB-SOA to reflect that it is an SOA factor related to biomass burning emissions.

2.2 Quantification of BrC absorptions

In Luo et al. (2022), we proposed an improved AAE ratio method to subtract brown carbon (BrC) absorptions from measured total aerosol absorptions during this field campaign. The details of this method can be found in Luo et al. (2022). We only introduce briefly the framework of the new method here. The essential part of deconvolving BrC absorptions from total aerosol absorptions is the adequate representation of black carbon (BC) spectral absorptions using the Ångström exponent law. Results of previous studies (Wang et al., 2018a; Li et al., 2019) demonstrated that the significant wavelength dependence of AAE_{BC} and the constant assumption of AAE_{BC} in BrC absorption retrievals might lead to significant bias. Thus, the AAE ratio defined as $R_{AAE}(\lambda) = AAE_{BC,\ \lambda-880}/AAE_{BC,\ 950-880}$ was proposed to tackle spectral AAE_{BC} variations, and online measurement data of $AAE_{950-880}$ were used as $AAE_{BC,\ 950-880}$ due to negligible absorption contributions of BrC at wavelengths of 880 and 950 nm. Thus, BrC absorptions (σ_{BrC}) at different wavelength (λ) including 370, 470, 530, 590, and 660 nm can be derived using the following formula, where σ_a is measured aerosol absorption.

$$\sigma_{BrC}(\lambda) = \sigma_a(\lambda) - \sigma_{BC}(880\,nm)$$
$$\times \left(\frac{880}{\lambda}\right)^{AAE_{BC,\ 950-880} \times R_{AAE}(\lambda)} \quad (1)$$

From the sophisticated discussions in Luo et al. (2022), variations in many factors such as BC refractive index, coating shell refractive index, BC mixing state, and BC mass size distributions (Li et al., 2019) influence the magnitudes of $R_{AAE}(\lambda)$. However, sensitivity tests shown in Luo et al. (2022) clearly concluded that BC mass size distributions dominated $R_{AAE}(\lambda)$ variations. In the Heshan campaign, the BC calibration for SP-AMS was not available. The carbon signals were used to retrieve the shape of the BC mass size distribution, and the total mass was constrained by the ratio between integrated C_x (C_1–C_9) signals and BC mass concentrations provided by the AE33. The real-time-measured carbon fragment (C_x) distributions by the SP-AMS were therefore used to distribute the total BC mass to different diameter bins (Eq. 8 in the supplement of Luo et al., 2022) to calculate $R_{AAE}(\lambda)$, as introduced in Luo et al. (2022). Details of the calculation can be found in their supplement. The average and standard deviations of R_{AAE} (370), R_{AAE} (470), R_{AAE} (520), R_{AAE} (590), and R_{AAE} (660) are 0.79 ($\pm$0.044), 0.85 ($\pm$0.038), 0.88 ($\pm$0.035), 0.9 ($\pm$0.035), and 0.93 ($\pm$0.031) during the observation period.

3 Results and discussions

3.1 Highly absorptive SOA formed during nighttime

As reported by Luo et al. (2022), biomass burning events happened frequently during the observation period and biomass burning was the dominant source of primary organic aerosols with the average BBOA/HOA ratio of 3.3. Significant contributions of BrC to total aerosol absorptions (Fig. S2a), together with the strong biomass burning emissions before dusk (Luo et al., 2022), provided a unique opportunity to explore the nighttime chemistry associated with biomass burning and its impacts on atmospheric BrC evolution in biomass burning plumes. Time series of retrieved $\sigma_{BrC,370}$ and BBOA are shown in Fig. 1a. It shows that BBOA varies quite consistently with $\sigma_{BrC,370}$ and they are highly correlated ($R = 0.88$; Fig. S2b), demonstrating the dominant contribution of BBOA to BrC absorptions. However, the correlation coefficient between BBOA and σ_{BrC} decreases as the wavelength increases; i.e., the correlation coefficients between σ_{BrC} at 470, 520, 590, and 660 nm and BBOA are 0.83, 0.8, 0.76, and 0.69 (Fig. S2b–f). In addition, as shown in Fig. 1a, coordinate variations between BBOA and $\sigma_{BrC,370}$ are usually seen during daytime, especially during the dusk BBOA spike periods. However, the $\sigma_{BrC,370}$ sometimes deviates substantially from BBOA variations during the nighttime (gray areas in Fig. 1). The average diurnal variations in both $\sigma_{BrC,370}$ and the ratio $\sigma_{BrC,370}$/BBOA are presented in Fig. 2a. Quick $\sigma_{BrC,370}$/BBOA increases were observed during nighttime before 06:00 LT. These results demonstrate that organic aerosol components other than BBOA might also contribute substantially to BrC absorption and differ much at different wavelengths as indicated by distinct correlations between BBOA and $\sigma_{BrC,370}$ at different wavelengths.

The time series of OA factors other than BBOA are also shown in Fig. 1b–d. As analyzed in Kuang et al. (2021), SOA contributes dominantly to total OA mass (SOA mass fraction > 70 % on average) during this field campaign. The most prominent features of SOA formations are the quick daytime formation of LOOA and BB-SOA and the nighttime formation of Night-OA, while MOOA exhibits almost no diurnal variations and are mostly associated with the regional air mass. The average mass absorption efficiencies (MAEs, defined as absorption coefficient per unit mass,
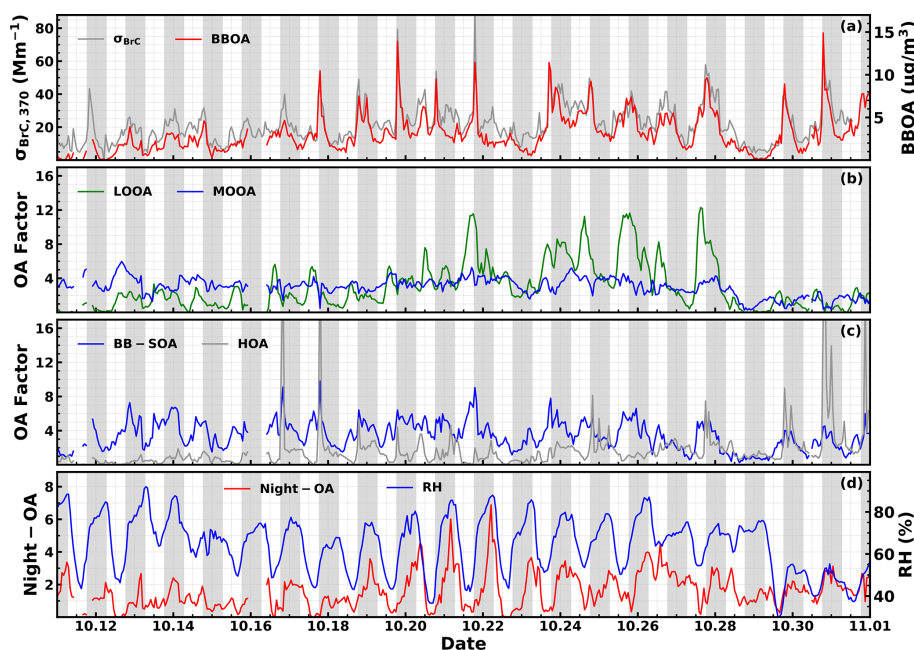
Figure 1. Time series of **(a)** brown carbon absorption at 370 nm ($\sigma_{\mathrm{BrC},370}$) on the left axis and BBOA on the right axis. **(b)** LOOA and MOOA, **(c)** BB-SOA and HOA, and **(d)** Night-OA on the left axis and RH on the right axis. Shaded areas represent nighttime periods.

$\mathrm{m^2\,g^{-1}}$) of different OA factors are retrieved using the multivariate linear regression method which is commonly used for this purpose (de Sá et al., 2019; Kasthuriarachchi et al., 2020). The multivariate linear regression method was expressed as $\sigma_{\mathrm{BrC}}(\lambda) = [\mathrm{HOA}] \times \mathrm{MAE}_{\mathrm{HOA}}(\lambda) + [\mathrm{MOOA}] \times \mathrm{MAE}_{\mathrm{MOOA}}(\lambda) + [\mathrm{LOOA}] \times \mathrm{MAE}_{\mathrm{LOOA}}(\lambda) + [\mathrm{BBOA}] \times \mathrm{MAE}_{\mathrm{BBOA}}(\lambda) + [\mathrm{Night\text{-}OA}] \times \mathrm{MAE}_{\mathrm{Night\text{-}OA}}(\lambda) + [\mathrm{BB\text{-}SOA}] \times \mathrm{MAE}_{\mathrm{BB\text{-}SOA}}(\lambda)$, where [OA factor] represents mass concentration and λ represents optical wavelength. Note that the MAE retrieval using the multilinear regression bears uncertainties and is affected by many factors; i.e., it is not completely independent of factors. The deduced average MAE values at 370 nm for BBOA, BB-SOA, HOA, LOOA, MOOA, and Night-OA are 3.8, 0.84, 0.24, 0, 1, and $2.3\,\mathrm{m^2\,g^{-1}}$, respectively (fitting performance was shown in Fig. S3). Note that negative value of about -0.1 is retrieved if LOOA values were inputs of the multivariate linear regressions, demonstrating quite low absorptivity of LOOA. Thus, the MAE of LOOA is treated as zero. As shown in Fig. 1b, rapid LOOA formation episodes happened frequently during daytime, but $\sigma_{\mathrm{BrC},370}$ still varies only with BBOA during that period, which confirms the white property of LOOA. The derived MAE of HOA is very small, which is consistent with the low absorptivity of HOA during HOA spikes. The prominent BrC factors are identified as BBOA, Night-OA, MOOA, and BB-SOA. The most surprising part is the highly absorptive property of Night-OA whose absorptivity is only lower than that of BBOA but much higher than other OA factors. Based on derived MAE values for OA factors as well as their mass concentrations, contributions of OA factors to

$\sigma_{\mathrm{BrC},370}$ are estimated and their diurnal variations are shown in Fig. 2b. It reveals that Night-OA accounts for the second largest contribution to BrC absorption during nighttime and even approaches the contribution of BBOA near 06:00 LT ($>30\,\%$), which explains the observed substantial nighttime deviation of $\sigma_{\mathrm{BrC},370}$ from BBOA as shown in Fig. 2a. The average contributions of BBOA, Night-OA, MOOA, and BB-SOA to $\sigma_{\mathrm{BrC},370}$ are 50 %, 20 %, 16 %, and 12 %, respectively. The time series of estimated OA contributions to BrC absorption at 370 nm are shown in Fig. S4, demonstrating that Night-OA sometimes even contributes dominantly ($>50\,\%$) to $\sigma_{\mathrm{BrC},370}$ especially when a rapid increase in Night-OA appeared during the night.

Different BrC components usually exhibit different absorption spectral dependences (Laskin et al., 2015). Diurnal variations in $\mathrm{AAE}_{370\text{-}470,\,\mathrm{BrC}}$ are investigated and shown in Fig. 2c. The $\mathrm{AAE}_{370\text{-}470,\,\mathrm{BrC}}$ exhibits distinct diurnal variations, with one peak at dusk when BBOA reaches its highest mass concentration and a trough at the time when Night-OA contributes most to and BBOA contribute the least to $\sigma_{\mathrm{BrC},370}$. This phenomenon suggests that spectral dependence of Night-OA absorptivity differs much from that of BBOA. The aforementioned multivariate linear regression method is thus also used for retrieving MAEs of BBOA and Night-OA at wavelengths of 470, 520, 590, and 660 nm. The overall fitting performance of using retrieved MAE values at multiple wavelengths is shown in Fig. S3. The retrieved spectral dependence of BBOA and Night-OA absorptivity is shown in Fig. 2d. The results show that Night-OA cloud likely absorbs as strongly as that of BBOA at visi-

ble wavelength ranges, suggesting a more important role of Night-OA in BrC absorption than expected from the retrieval of $\sigma_{BrC,370}$. The retrieved $AAE_{370–470}$ and $AAE_{470–590}$ for BBOA are 3 and 5.9 and for Night-OA 1.3 and 6, which explains the observed quick decrease in $AAE_{370–470,\,BrC}$ during nighttime. The direct quantification of $AAE_{370–470}$ and $AAE_{470–590}$ for BBOA is difficult due to the entanglement of BC absorption and is thus rarely reported. The retrieved $AAE_{470–590}$ for BBOA and Night OA is in general consistent with the AAE of bulk BrC solutions ($AAE_{300–600}$ of near 6) extracted using different solvents which were sampled during and after a nighttime nationwide biomass burning event (Lin et al., 2017).

The Night-OA was named because of its prominent night increase (Fig. 3a) and has previously been speculated as being secondary because of its tight correlation with nitrate. However, Night-OA has a relatively low O/C ratio of 0.32, raising the question of whether it originates from primary emissions or secondary formation. As discussed in Luo et al. (2022), traffic, cooking (the HOA and cooking-related OA were not separated in the PMF results, although the hydrocarbon-like factor was named HOA as discussed in Kuang et al., 2021), and biomass burning are likely the dominant primary sources during this campaign. If Night-OA was a primary source, it would be expected to increase alongside other primary sources. We identified most Night-OA increase events and examined their correlation with variations in other primary sources, as shown in Fig. 3b–e. This analysis reveals that Night-OA increases were typically observed after sunset, though occasionally during the daytime. Night-OA increases showed weak correlations with changes in CO ($R = 0.25$), HOA ($R = 0.1$), and BBOA ($R = -0.15$) but a moderate correlation with NO_x ($R = 0.55$). During significant biomass burning events (indicated by substantial BBOA increases), the concentration of Night-OA decreased on average (Fig. 3 of Luo et al., 2022), suggesting that Night-OA is unlikely to be emitted from biomass burning. We also identified all significant HOA increase events that did not coincide with biomass burning and analyzed the average HOA increase and variations in other aerosol components (Fig. S2). It shows that, despite significant HOA increases, the average mass concentration of Night-OA remained almost unchanged, indicating that Night-OA is also unlikely to originate from HOA-associated emissions. Therefore, the weak but positive correlations between Night-OA and HOA as well as CO are likely associated with the accumulation characteristics of primary emissions after sunset. The higher correlations between Night-OA and NO_x may also result from the accumulation of NO_x starting in the afternoon when photochemical depletion is weaker. Another possibility to consider is whether Night-OA increases could be associated with plumes containing higher NO_x transported from other regions. We investigated the diurnal variations in the Night-OA/CO and Night-OA/NO_x ratios. If Night-OA was transported together with NO_x, their ratio would retain char-

acteristics such as remaining near constant. However, persistent increases in Night-OA/CO and Night-OA/NO_x ratios were observed when significant Night-OA formation began. This suggests that Night-OA is likely formed through secondary processes that would result in a ratio increase in Night-OA for both NO_x and CO, consistent with its being also correlated with nitrate ($R = 0.67$). The low O/C of Night-OA, still higher than that of the primary factor HOA, was determined by a high amount of $C_xH_y^+$ ions. However, the Night-OA was also characterized by the significant intensity of oxidation tracers $C_2H_3O^+$ and CO_2^+, suggesting that Night-OA was an oxidation product with a low oxidation state during the nighttime. A similar situation was previously found in a study at Bakersfield, USA, in which Liu et al. (2012) identified SOA factors as alkane SOA and aromatic SOA with moderate O/C (0.27–0.36). Simultaneously, NO_x potentially promoted its formation, given the highest N/C ratio of Night-OA among all resolved factors. This will be discussed further in Sect. 3.2.

3.2 Precursors and possible mechanisms of the Night-OA formation

As shown in Figs. 1a and 2d, the Night-OA concentration increased during the nighttime and usually decreased and reached near zero in the afternoon. Therefore, the Night-OA factor is characterized by its rapid nighttime formation and quick daytime loss (through practices like repartitioning and photodegradation). In general, SOA can be formed either through condensation of gas-phase chemically aged low- or semi-volatile VOC precursors following the gas–particle partitioning theory (Odum et al., 1996) or in the aqueous phase through further oxidation of water-soluble primary VOCs as well as secondary products of gas-phase VOC aging processes (Blando and Turpin, 2000; Ervens et al., 2011), with the former referred to as gasSOA and the latter referred to as aqSOA (Kuang et al., 2020a). Recent research has revealed that SOA can also be formed through the oxidation of semi-volatile components evaporated from emitted primary organic aerosols in the gas phase (Palm et al., 2020) or in the aqueous phase (Wang et al., 2021). Considering the highly absorptive characteristics of secondarily formed Night-OA, exploring the sources and formation pathways of Night-OA is of great importance in evaluating the importance of Night-OA formations in the global atmosphere.

3.2.1 Evidence of biomass burning emissions as precursor source of Night-OA formation

The VOC profiles of this observation site are quite complex as mixtures of both different anthropogenic sources and natural sources (Song et al., 2019). However, prominent and continuous Night-OA formation events observed from 19 to 22 October which are accompanied by frequently observed sharp increases in BBOA mass concentrations at nightfall of-
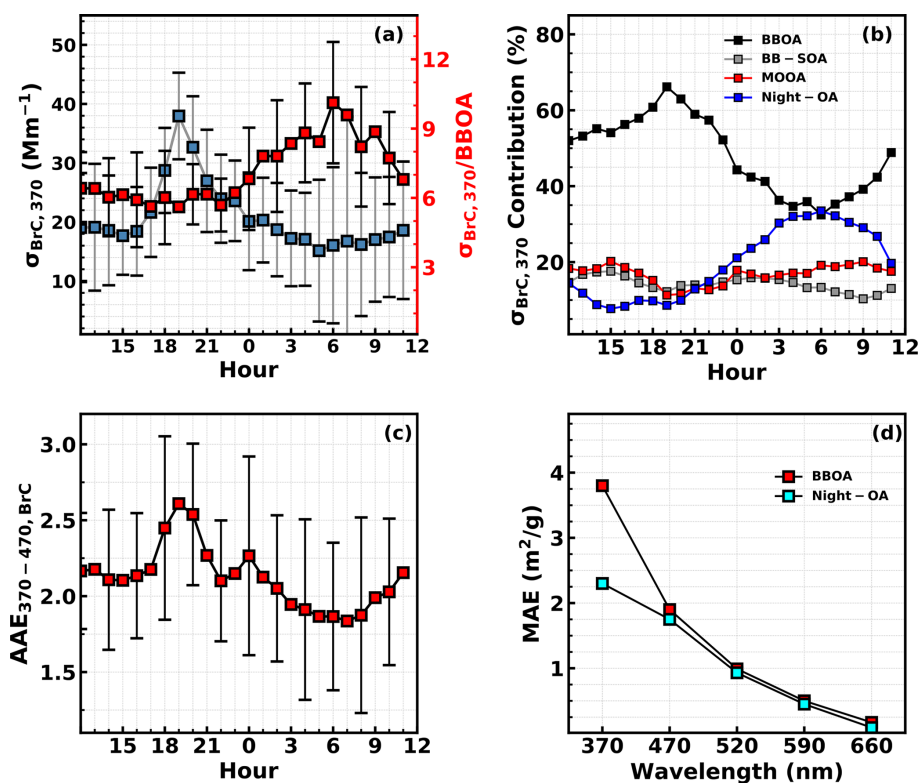
Figure 2. (a) Diurnal variations in $\sigma_{\text{BrC},370}$ and the ratio $\sigma_{\text{BrC},370}/$BBOA. **(b)** Diurnal variations in contributions of different OA factors to $\sigma_{\text{BrC},370}$. **(c)** Average diurnal variations in brown carbon absorption Ångström exponent between 370 and 470 nm. **(d)** Retrieved mass absorption efficiencies (MAEs) of BBOA and Night-OA at multiple wavelengths using the multilinear regression model.
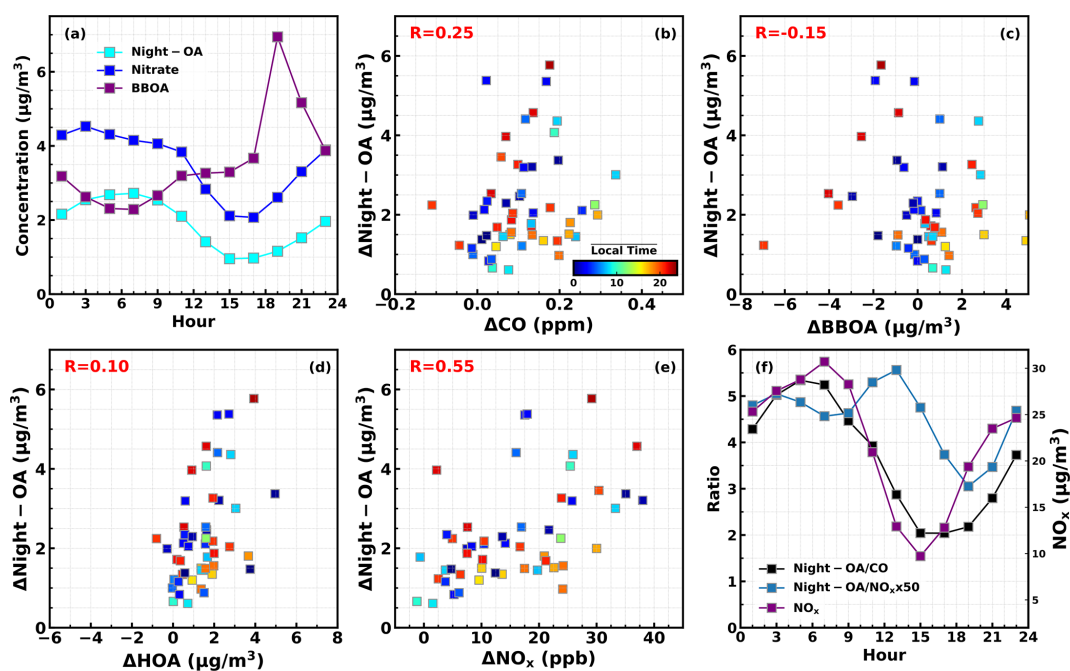

Figure 3. (a) Diurnal variations in nitrate, Night-OA, and BBOA. **(b)–(e)** Relations between increases in Night-OA and increases in CO, BBOA, HOA, and NO_x for identified Night-OA increase cases; colors of scatter plots represent the average local time of Night-OA increase cases. **(f)** Diurnal variations in the ratios Night-OA/CO and Night-OA/NO_x on the left axis and NO_x on the right axis.

fer hints that Night-OA formation might be associated with biomass burning emissions. Indeed, the air is always in motion and behaves in a Lagrangian manner. Although the observation location is fixed, the information collected at different times corresponds to signals from different air parcels. However, if the biomass burning events are regionally representative, the relationship between the observed increase in Night-OA signals after midnight and the biomass burning emission signals before midnight may still provide valuable insights. The average nighttime mass concentrations of Night-OA from 22:00 to 06:00 LT (the next day) are plotted against the average BBOA mass concentrations from 16:00 to 22:00 LT of this campaign, and the results are shown in Fig. 4a. It shows that Night-OA formation is positively correlated with BBOA from the night before, which supports the speculation that Night-OA formation is a result of the nighttime chemistry of biomass burning emissions. The nighttime oxidant levels indicated by the concentrations of O_x ($NO_2 + O_3$) represented by colors in Fig. 4a demonstrate that the highest Night-OA formation was accompanied by the strongest biomass burning emissions and the most abundant oxidants, suggesting the importance of nighttime aging processes in Night-OA formation. The following evidence shows that gas-phase and aqueous-phase chemistries of biomass burning precursors likely have coordinated to promote the quick nighttime formation of Night-OA.

3.2.2 Evidence of nighttime multiphase processes that promoted Night-OA formation

Three obvious Night-OA formation episodes which lasted more than 3 d, as shown in Fig. S6, were observed during the entire field campaign. The peak Night-OA mass concentration of each night increased during these episodes and was accompanied by an increase in nighttime peak RH during each episode, suggesting that abundant nighttime aerosol water might play a significant role in Night-OA formation. More solid clues could be found from different behaviors of gas-SOA and aqSOA formations in modifying the aerosol size distribution. The gasSOA forms through condensation following partitioning theory, thus adding mass mainly to the condensation mode which contributes most to aerosol surface area concentrations (Kuang et al., 2020a; Zhai et al., 2023), whereas aqSOA formation depends on the amount of liquid water content, thus adding mass mainly to the mode where most aerosol water resides. The evolution of the average OA size distribution during the night of 20 and 21 October when the most prominent Night-OA formation occurred is illustrated in Fig. 4b. During the two nights from 22:00 to 06:00 LT, Night-OA formations contributed most to the mass concentration increase of all OA, and HOA contributed less, while mass concentrations of all other OA factors decreased and partially balanced out the OA increase (Fig. 4c). HOA emissions mainly added mass to the diameter ranges of 100–300 nm as demonstrated by Luo et al. (2022). However, as

shown in Fig. 4b, a substantial increase in mass concentrations at a diameter range >300 nm occurred. All other SOA factors even showed a decreasing trend for the case shown in Fig. 4c, suggesting that the substantial OA mass increases larger than 300 nm are being contributed by the Night-OA increase. The results shown in Fig. 4d demonstrate that the size-resolved increase in OA mass for the abovementioned cases (Fig. 4b and c) was highly correlated with size-resolved aerosol liquid water content (details about the size-resolved aerosol water content calculation are presented in Sect. S1 of the Supplement), demonstrating that the Night-OA formation added mass mainly to aerosol water-abundant diameter ranges. The average RH of the cases shown in Fig. 4b–d is around 80 %, with a corresponding average hygroscopicity parameter κ of 0.26 measured by the humidified nephelometer system, demonstrating a growth factor of ~ 1.27 (water thickness of ~ 81 nm for aerosol diameter of about 300 nm), thus not a thin film of water for heterogeneous reactions, but it more likely formed through dark aqueous reactions. Primary biomass burning aerosols are nearly hydrophobic under subsaturated conditions due to abundant organics (Kuang et al., 2024; Tao et al., 2024), meaning that multiphase chemistry involving preexisting background hygroscopic aerosols plays a significant role in the aging of biomass burning plumes.

In addition, as shown in Fig. S7, the Night-OA decreased quickly during daytime, which is beyond the dilution effect of boundary layer development (indicated by rapid decrease in Night-OA/CO as shown in Fig. S7). The substantial daytime loss of Night-OA which might be caused by several processes, such as partitioning evaporation, photodegradation (Wang et al., 2023b), and chemical transformations. The partitioning dynamics of gasSOA and aqSOA also differ much, which might add more information when looking into the Night-OA formation pathway. Following the rule of partitioning theory, the evaporation equilibrium of the condensation of gasSOA is tightly associated with air temperature. Equilibrium of the reversible aqSOA formation greatly depends on aerosol water changes, while evaporation of irreversible SOA production through aqueous pathways is quite sophisticated (Tong et al., 2021). It was found that the percentile of Night-OA mass loss during the daytime (07:00 to 16:00 LT) is more tightly correlated with RH decrease compared with temperature increase (Fig. S8). HOA also exhibits obvious evaporation during daytime (indicated by a rapid decrease in HOA/CO; Fig. S7); however, the daytime loss of HOA seems more tightly correlated with temperature increase as shown in Fig. S9. The phenomenon that Night-OA daytime loss is more correlated with RH decrease implied that part of Night-OA possibly co-evaporated with water vapor as RH decreases. This might serve as a weak but still supportive clue for how Night-OA was likely formed through aqueous pathways and is maybe reversible.

As revealed by Fig. 4a – that nighttime oxidation levels play a significant role in Night-OA formation – the question
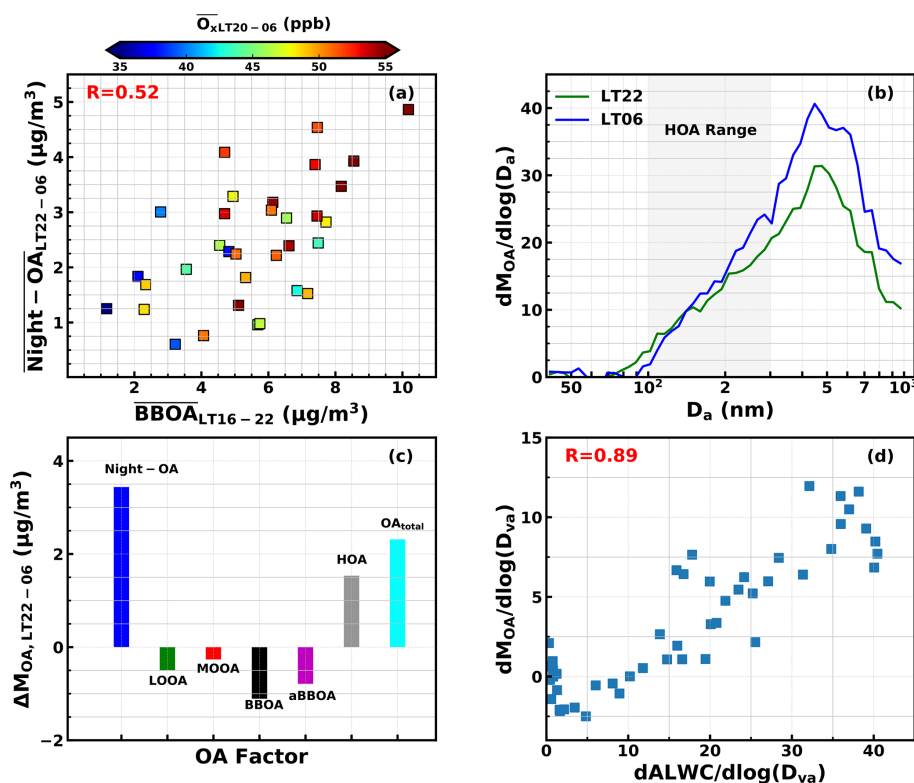
Figure 4. (a) Correlations between average nighttime Night-OA mass concentrations and average BBOA mass concentrations over LT16–22 (local time 16:00 to 22:00 LT), the colors corresponding to the average O_x ($NO_2 + O_3$) mixing ratio (ppb) during the night. **(b)** Average evolutions of organic aerosol mass size distributions from local time 22:00 (20, 21 October) to 06:00 (21, 22 October), the gray band showing the size range of 100–300 nm. **(c)** Average differences for organic aerosol (OA) mass concentration corresponding to **(b)**. **(d)** The correlations between the increase in size-resolved organic mass concentrations in **(c)** (LT06 minus LT22: local time 06:00 minus local time 22:00) with average size-resolved aerosol liquid water content (ALWC).

of the role of nighttime gas-phase chemistry in promoting the Night-OA formation is left open.

The average diurnal variations in gas pollutants and meteorological parameters typical of nighttime chemistry including NO, NO_2, O_3, Night-OA, nitrate, RH, and BBOA for the most prominent Night-OA formation case (20 to 21 October, consistent with Fig. 4b) are shown in Fig. 5. At night, NO_2 and NO_3 radicals do not photolyze. NO reacts rapidly with O_3, and as a result almost all NO_x is converted to NO_2 (Fig. 5a). NO_2 will further react with O_3 to form the NO_3 radical, which is the most important gas-phase oxidant during the nighttime (Chapleski et al., 2016). In this case, NO_2 concentration increased substantially before the sunset, but the trend ended and shifted suddenly to a decrease when BBOA emissions were highest and then decreased rapidly along with the dropping BBOA mass concentration. The reduction in BBOA mass concentration mainly attributed to the end of local combustion events might also be associated with BBOA evaporation after its strong emissions due to the mix of biomass burning plumes with background air mass. This dilution effect shall deliver semi-volatile VOCs such as phenolic compounds from the particle phase to gas phase (Palm

et al., 2020). The Night-OA increased slowly during the rapid NO_2 decrease phase, but the nitrate concentration increased substantially with decreasing O_3 concentration (still higher than 30 ppb as shown in gray shaded areas). The hydrolysis of N_2O_5 (Evans and Jacob, 2005; Bertram and Thornton, 2009; Wang et al., 2017; Chen et al., 2018; Wang et al., 2020) that is formed from the NO_2 addition of NO_3 radicals (Seinfeld and Pandis, 2016; Fan et al., 2022) represents an important pathway of nitrate formation during the nighttime period. The rapid decrease in NO_2 coincident with the quick nitrate formation implies that the rapid NO_2 consumption supplied the NO_3 and N_2O_5 reaction chains (Yang et al., 2022; Wang et al., 2023a), providing abundant NO_3 radicals during the initial stage of Night-OA formation and likely initialized the Night-OA formation (Rollins et al., 2012; Kiendler-Scharr et al., 2016; Decker et al., 2019). The active nighttime NO_3 chemistry and its impacts on nitrate formations during the observation periods were further confirmed by Yang et al. (2022), who conducted box model simulations. In addition, Li et al. (2020a) demonstrated that night NO_3 radicals darkened the BBOA with the MAE enhancement ratio range from 1.3 to 3.2 for optical wavelengths of less than 650 nm.
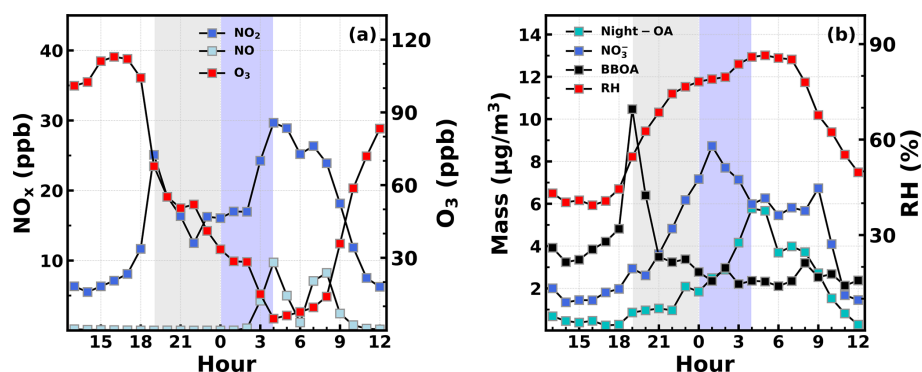
Figure 5. Average diurnal variations in **(a)** NO_2, NO, and O_3 and **(b)** Night-OA, nitrate, BBOA, and RH during the two nights – 20 to 21 October – when the most prominent Night-OA formation occurred. Shaded areas represent periods of Night-OA increase, and blue parts correspond to the remarkable increase period of Night-OA.

The retrieved average MAE of BBOA through multilinear fitting was higher than the average MAE of freshly emitted BBOA during BBOA spikes as reported by Luo et al. (2022) (3.8 vs. 2.6 $m^2 g^{-1}$). This result suggests the possible darkening of primary BBOA, which is consistent with the prevailing nighttime NO_3 chemistry processes during the observations (Yang et al., 2022). The highest Night-OA production rate occurred when both NO_2 and NO began to increase (O_3 still decreased rapidly and reached below 30 ppb, shown as the blue shaded area) and the RH reached near its maximum. These characteristics further highlight the crucial role of aerosol liquid water content in Night-OA formation. However, the quick increase in NO_2 and NO implies that the dominant contribution of NO_2 formation to O_3 depletion (Wang et al., 2023a) was during the quick Night-OA increase stage. At this stage, the NO_3 radical chemistry have ceased and likely did not directly participate in the succeeding quick aqueous-phase Night-OA formation. Nevertheless, the quick depletion of O_3 and the increase in NO_2 with the quickest Night-OA formation occurred demonstrate that the NO_2 might play a significant role in the subsequent quick Night-OA formation. These results demonstrate that the aqueous-phase processing of biomass burning emissions with abundant NO_2 could likely form highly absorptive SOA, while the nighttime gas-phase chemistry with typically high NO_2, NO_3 radicals, and RH could likely magnify the Night-OA formation.

A previous field study (Lin et al., 2017) demonstrated that most chromophores were nitroaromatic compounds (NACs) during the observed nighttime bonfire event with the major contribution to the solvent-extractable BrC. In this study, the NAC contribution to BrC absorption increased towards near-visible wavelengths, and this characteristic is consistent with the aforementioned BrC absorption spectral dependence characteristics in Sect. 3.1. Actually, the relatively low O/C of Night-OA and high N/C and H/C ratios (0.04 and 1.89, even higher than those of BBOA which are known to be composed of complex nitrogen-containing compounds)

were consistent with the features (low O/C, high N/C (ring- and N-containing structures of NACs), and low hygroscopicity) of aerosols that involved such nitro-phenolic compounds (Chen et al., 2022). These compounds are secondarily formed from reactions of cyclic aromatics that involve NO_3 radical chemistry (Rana and Guzman, 2022; Mayorga et al., 2021) during nighttime which likely have larger molecular weight and thereby lower hygroscopicity (Wang et al., 2019a; Price et al., 2022; Petters et al., 2009). The increased loading of Night-OA would lower organic aerosol hygroscopicity, which was confirmed previously by Kuang et al. (2021). The high N/C of Night-OA was consistent with its strong absorptivity considering that aerosol absorptions are generally linked with N-containing components (Qin et al., 2018; Kasthuriarachchi et al., 2020). However, an N/C of 0.04 implies the complex structures of Night-OA components. These results also demonstrate that NACs are probably key components of the Night-OA factor, considering that biomass burning was indeed an important source of precursors (Li et al., 2020b; Decker et al., 2019) in forming NACs. This is consistent with the inference that precursors of Night-OA came from biomass burning. On the basis of the limited existing literature, Wang et al. (2019c) have summarized the secondary NAC formation pathways of benzene, toluene, phenol, and methylcatechol which represented a significant fraction of biomass burning VOC emissions (Stockwell et al., 2015). Their findings emphasized that the NO_3 radical does not directly participate in the aqueous-phase reactions in NAC formation reaction chains but first oxidizes these precursors into intermediate products which then react with NO_2 to form nitrophenols and nitrocatechols that are further oxidized in the particle phase to generate NACs. This gas-phase oxidation and the subsequent particle-phase reaction chains of NAC production may explain the observed Night-OA formation characteristics in that the most-prominent Night-OA formation occurred after the strongest NO_3 radical chemistry when the aerosol liquid water content was abundant, therefore highlighting the great importance of nighttime multi-

phase chemistry in Night-OA formation. Aside from the case shown in Fig. 5, a much higher correlation coefficient between nighttime average Night-OA mass concentration and nighttime average O_x concentrations than that of NO_2 shown in Fig. S10 for the entire campaign (0.58 vs. 0.39) was revealed. This result further stresses that the coordination of nighttime gas-phase and aqueous-phase chemistry was responsible for the quick Night-OA formation. In addition, obvious daytime increase in Night-OA was occasionally observed (Figs. S11 and S12), as mentioned in Sect. 2 when the RH remained high and NO_2 and biomass burning emissions increased substantially. These results further emphasize that NO_2 might play a significant role in aqueous-phase reactions of oxidized biomass burning precursors which might be directly emitted or transformed through active nighttime NO_3 chemistry (Decker et al., 2019).

4 Environmental and climate significance

Biomass burning emissions, as one of the largest sources of primary aerosols and the second largest source of VOCs, have an increasingly greater impact on the regional air quality and global climate under the context of global warming (Running, 2006). However, the lack of knowledge on the complex chemical aging of biomass burning plumes during its transport hinders the accurate representation of biomass burning VOCs and BBOA evolution in air quality and climate models. Kodros et al. (2022) concluded based on laboratory experiments that the dark aging of biomass burning emissions was sensitive to RH. Their results suggested that the SOA was mainly formed through the condensation of gas-phase oxidation products, however, not ruling out the possibility of heterogeneous oxidations. This study highlights that nighttime gas-phase chemistry of biomass burning VOC precursors in conjunction with further aqueous-phase reactions likely contributed substantially to ambient SOA that is highly absorptive. Although more comprehensive studies about detailed mechanisms are needed and the robustness of the conclusion in this study needs to be further examined, the exact types of fires during this campaign are not known. Still, this finding has important implications for our understanding of the nighttime evolution of biomass burning plumes. Field observations in this study revealed the abundant existence of highly hygroscopic inorganic components within ambient aerosols that contributed substantially to aerosol liquid water in ambient air, while aerosols produced in the chamber of Kodros et al. (2022) were dominated by organics (only with very small amounts of inorganic nitrate formed during the aging processes) which might have inhibited aqueous reaction pathways. Inspired by this study, future laboratory studies investigating the nighttime aging of biomass burning plumes should consider not only the high nighttime RH conditions, but also the complex mixture of background

hygroscopic aerosols with biomass burning emissions when simulating aerosols within biomass burning plumes.

In addition, biomass burning plumes might form convective clouds under strong ground surface heating and moisture release (pyrocumulus clouds or pyrocumulonimbus clouds) (Andreae et al., 2004; Fromm et al., 2006; Cunningham and Reeder, 2009; Lareau and Clements, 2016) or interact with clouds and/or fogs during long-range transport (Engelhart et al., 2011). Clouds and fogs provide large amount of liquid water regardless of day or night, while active photochemistry in biomass burning plumes may increase O_3 and NO_2 production (Hecobian et al., 2011; Marufu et al., 2000; Ziemke et al., 2009) (biomass burning also emits NO_2 directly as shown in Fig. 5), likely promoting NO_3 radical production (Selimovic et al., 2020) during nighttime. This suggests a potential formation of highly absorptive SOA in cloud droplets, which results in even browner cloud droplets, impacting cloud optical properties, cloud lifetime (e.g., promoting cloud burning-off effect), and precipitation. Especially since violent pyroconvection can penetrate the stratosphere, the darkening of clouds might have regional impacts on cloud properties as well as radiative balance. Moreover, the biomass burning plumes transported from remote areas can sometimes mix down into the boundary layer and have a significant impact on regional air quality (Wang et al., 2018b). The top of the boundary layer is usually characterized by high-RH conditions due to abundant water vapor but lower temperatures (Kuang et al., 2016), as well as high O_x concentrations due to substantial anthropogenic NO_x emissions and active photochemistry. Thus, potentially large amounts of highly absorptive SOA formation could be expected in this kind of biomass burning plumes.

Overall, results of this study provide important insights into nighttime evolutions of biomass burning and an uncovered potential secondary BrC formation mechanism that has broad implications for climate and air quality effects of biomass burning, especially the possible interaction between biomass burning plumes with clouds in the aging process during nighttime. However, much more effort is still required to further disentangle the complex routes of gas-phase biomass burning VOC oxidation and subsequent aqueous-phase reactions. Current laboratory studies or box model simulations have not considered the important role played by preexisting background aerosols in the aging of biomass burning plumes. Preexisting background aerosols are generally much more hygroscopic that aerosols directly emitted from biomass burning emissions. Clues like this are indeed important for future laboratory studies that aim to disentangle important reactions and mechanisms that matter for biomass burning aging and corresponding SOA formation.

References

Ahern, A. T., Robinson, E. S., Tkacik, D. S., Saleh, R., Hatch, L. E., Barsanti, K. C., Stockwell, C. E., Yokelson, R. J., Presto, A. A., Robinson, A. L., Sullivan, R. C., and Donahue, N. M.: Production of Secondary Organic Aerosol During Aging of Biomass Burning Smoke From Fresh Fuels and Its Relationship to VOC Precursors, J. Geophys. Res.-Atmos., 124, 3583–3606, https://doi.org/10.1029/2018JD029068, 2019.

Akagi, S. K., Yokelson, R. J., Wiedinmyer, C., Alvarado, M. J., Reid, J. S., Karl, T., Crounse, J. D., and Wennberg, P. O.: Emission factors for open and domestic biomass burning for use in atmospheric models, Atmos. Chem. Phys., 11, 4039–4072, https://doi.org/10.5194/acp-11-4039-2011, 2011.

Andreae, M. O.: Emission of trace gases and aerosols from biomass burning – an updated assessment, Atmos. Chem. Phys., 19, 8523–8546, https://doi.org/10.5194/acp-19-8523-2019, 2019.

Andreae, M. O. and Gelencsér, A.: Black carbon or brown carbon? The nature of light-absorbing carbonaceous aerosols, Atmos. Chem. Phys., 6, 3131–3148, https://doi.org/10.5194/acp-6-3131-2006, 2006.

Andreae, M. O. and Merlet, P.: Emission of trace gases and aerosols from biomass burning, Global Biogeochem. Cy., 15, 955–966, https://doi.org/10.1029/2000GB001382, 2001.

Andreae, M. O., Rosenfeld, D., Artaxo, P., Costa, A. A., Frank, G. P., Longo, K. M., and Silva-Dias, M. A. F.: Smoking Rain Clouds over the Amazon, Science, 303, 1337–1342, https://doi.org/10.1126/science.1092779, 2004.

Bertram, T. H. and Thornton, J. A.: Toward a general parameterization of N_2O_5 reactivity on aqueous particles: the competing effects of particle liquid water, nitrate and chloride, Atmos. Chem. Phys., 9, 8351–8363, https://doi.org/10.5194/acp-9-8351-2009, 2009.

Bertrand, A., Stefenelli, G., Jen, C. N., Pieber, S. M., Bruns, E. A., Ni, H., Temime-Roussel, B., Slowik, J. G., Goldstein, A. H., El Haddad, I., Baltensperger, U., Prévôt, A. S. H., Wortham, H., and Marchand, N.: Evolution of the chemical fingerprint of biomass burning organic aerosol during aging, Atmos. Chem. Phys., 18, 7607–7624, https://doi.org/10.5194/acp-18-7607-2018, 2018.

Blando, J. D. and Turpin, B. J.: Secondary organic aerosol formation in cloud and fog droplets: a literature evaluation of plausibility, Atmos. Environ., 34, 1623–1632, https://doi.org/10.1016/S1352-2310(99)00392-1, 2000.

Bluvshtein, N., Lin, P., Flores, J. M., Segev, L., Mazar, Y., Tas, E., Snider, G., Weagle, C., Brown, S. S., Laskin, A., and Rudich, Y.: Broadband optical properties of biomass-burning aerosol and identification of brown carbon chromophores, J. Geophys. Res.-Atmos., 122, 5441–5456, https://doi.org/10.1002/2016JD026230, 2017.

Chapleski, R. C., Zhang, Y., Troya, D., and Morris, J. R.: Heterogeneous chemistry and reaction dynamics of the atmospheric oxidants, O_3, NO_3, and OH, on organic surfaces, Chem. Soc. Rev., 45, 3731–3746, https://doi.org/10.1039/c5cs00375j, 2016.

Chen, Y., Wolke, R., Ran, L., Birmili, W., Spindler, G., Schröder, W., Su, H., Cheng, Y., Tegen, I., and Wiedensohler, A.: A parameterization of the heterogeneous hydrolysis of N_2O_5 for mass-based aerosol models: improvement of particulate nitrate prediction, Atmos. Chem. Phys., 18, 673–689, https://doi.org/10.5194/acp-18-673-2018, 2018.

Chen, Y., Zheng, P., Wang, Z., Pu, W., Tan, Y., Yu, C., Xia, M., Wang, W., Guo, J., Huang, D., Yan, C., Nie, W., Ling, Z., Chen, Q., Lee, S., and Wang, T.: Secondary Formation and Impacts of Gaseous Nitro-Phenolic Compounds in the Continental Outflow Observed at a Background Site in South China, Environ. Sci. Technol., 56, 6933–6943, https://doi.org/10.1021/acs.est.1c04596, 2022.

Cheng, Z., Atwi, K. M., Yu, Z., Avery, A., Fortner, E. C., Williams, L., Majluf, F., Krechmer, J. E., Lambe, A. T., and Saleh, R.: Evolution of the light-absorption properties of combustion brown carbon aerosols following reaction with nitrate radicals, Aerosol Sci. Tech., 54, 849–863, https://doi.org/10.1080/02786826.2020.1726867, 2020.

Cunningham, P. and Reeder, M. J.: Severe convective storms initiated by intense wildfires: Numerical simulations of pyro-convection and pyro-tornadogenesis, Geophys. Res. Lett., 36, L12812, https://doi.org/10.1029/2009GL039262, 2009.

de Sá, S. S., Rizzo, L. V., Palm, B. B., Campuzano-Jost, P., Day, D. A., Yee, L. D., Wernis, R., Isaacman-VanWertz, G., Brito, J., Carbone, S., Liu, Y. J., Sedlacek, A., Springston, S., Goldstein, A. H., Barbosa, H. M. J., Alexander, M. L., Artaxo, P., Jimenez, J. L., and Martin, S. T.: Contributions of biomass-burning, urban, and biogenic emissions to the concentrations and light-absorbing properties of particulate matter in central Amazonia during the dry season, Atmos. Chem. Phys., 19, 7973–8001, https://doi.org/10.5194/acp-19-7973-2019, 2019.

Decker, Z. C. J., Zarzana, K. J., Coggon, M., Min, K.-E., Pollack, I., Ryerson, T. B., Peischl, J., Edwards, P., Dubé, W. P., Markovic, M. Z., Roberts, J. M., Veres, P. R., Graus, M., Warneke, C., de Gouw, J., Hatch, L. E., Barsanti, K. C., and Brown, S. S.: Nighttime Chemical Transformation in Biomass Burning Plumes: A Box Model Analysis Initialized with Aircraft Observations, Environ. Sci. Technol., 53, 2529–2538, https://doi.org/10.1021/acs.est.8b05359, 2019.

Drinovec, L., Močnik, G., Zotter, P., Prévôt, A. S. H., Ruckstuhl, C., Coz, E., Rupakheti, M., Sciare, J., Müller, T., Wiedensohler, A., and Hansen, A. D. A.: The "dual-spot" Aethalometer: an improved measurement of aerosol black carbon with real-time loading compensation, Atmos. Meas. Tech., 8, 1965–1979, https://doi.org/10.5194/amt-8-1965-2015, 2015.

Engelhart, G. J., Moore, R. H., Nenes, A., and Pandis, S. N.: Cloud condensation nuclei activity of isoprene secondary organic aerosol, J. Geophys. Res.-Atmos., 116, D02207, https://doi.org/10.1029/2010jd014706, 2011.

Ervens, B., Turpin, B. J., and Weber, R. J.: Secondary organic aerosol formation in cloud droplets and aqueous particles (aq-SOA): a review of laboratory, field and model studies, Atmos. Chem. Phys., 11, 11069–11102, https://doi.org/10.5194/acp-11-11069-2011, 2011.

Evans, M. J. and Jacob, D. J.: Impact of new laboratory studies of N2O5 hydrolysis on global model budgets of tropospheric nitrogen oxides, ozone, and OH, Geophys. Res. Lett., 32, L09813, https://doi.org/10.1029/2005GL022469, 2005.

Fan, M.-Y., Zhang, Y.-L., Lin, Y.-C., Hong, Y., Zhao, Z.-Y., Xie, F., Du, W., Cao, F., Sun, Y., and Fu, P.: Important Role of NO_3 Radical to Nitrate Formation Aloft in Urban Beijing: Insights from Triple Oxygen Isotopes Measured at the Tower, Environ. Sci. Technol., 56, 6870–6879, https://doi.org/10.1021/acs.est.1c02843, 2022.

Fromm, M., Tupper, A., Rosenfeld, D., Servranckx, R., and McRae, R.: Violent pyro-convective storm devastates Australia's capital and pollutes the stratosphere, Geophys. Res. Lett., 33, L05815, https://doi.org/10.1029/2005GL025161, 2006.

Hartikainen, A., Yli-Pirilä, P., Tiitta, P., Leskinen, A., Kortelainen, M., Orasche, J., Schnelle-Kreis, J., Lehtinen, K. E. J., Zimmermann, R., Jokiniemi, J., and Sippula, O.: Volatile Organic Compounds from Logwood Combustion: Emissions and Transformation under Dark and Photochemical Aging Conditions in a Smog Chamber, Environ. Sci. Technol., 52, 4979–4988, https://doi.org/10.1021/acs.est.7b06269, 2018.

Hecobian, A., Liu, Z., Hennigan, C. J., Huey, L. G., Jimenez, J. L., Cubison, M. J., Vay, S., Diskin, G. S., Sachse, G. W., Wisthaler, A., Mikoviny, T., Weinheimer, A. J., Liao, J., Knapp, D. J., Wennberg, P. O., Kürten, A., Crounse, J. D., Clair, J. St., Wang, Y., and Weber, R. J.: Comparison of chemical characteristics of 495 biomass burning plumes intercepted by the NASA DC-8 aircraft during the ARCTAS/CARB-2008 field campaign, Atmos. Chem. Phys., 11, 13325–13337, https://doi.org/10.5194/acp-11-13325-2011, 2011.

Hodshire, A. L., Akherati, A., Alvarado, M. J., Brown-Steiner, B., Jathar, S. H., Jimenez, J. L., Kreidenweis, S. M., Lonsdale, C. R., Onasch, T. B., Ortega, A. M., and Pierce, J. R.: Aging Effects on Biomass Burning Aerosol Mass and Composition: A Critical Review of Field and Laboratory Studies, Environ. Sci. Technol., 53, 10007–10022, https://doi.org/10.1021/acs.est.9b02588, 2019.

Jiang, H., Frie, A. L., Lavi, A., Chen, J. Y., Zhang, H., Bahreini, R., and Lin, Y.-H.: Brown Carbon Formation from Nighttime Chemistry of Unsaturated Heterocyclic Volatile Organic Compounds, Environ. Sci. Tech. Let., 6, 184–190, https://doi.org/10.1021/acs.estlett.9b00017, 2019.

Jo, D. S., Park, R. J., Lee, S., Kim, S.-W., and Zhang, X.: A global simulation of brown carbon: implications for photochemistry and direct radiative effect, Atmos. Chem. Phys., 16, 3413–3432, https://doi.org/10.5194/acp-16-3413-2016, 2016.

Kasthuriarachchi, N. Y., Rivellini, L.-H., Adam, M. G., and Lee, A. K. Y.: Light Absorbing Properties of Primary and Secondary Brown Carbon in a Tropical Urban Environment, Environ. Sci. Technol., 54, 10808–10819, https://doi.org/10.1021/acs.est.0c02414, 2020.

Kiendler-Scharr, A., Mensah, A. A., Friese, E., Topping, D., Nemitz, E., Prevot, A. S. H., Äijälä, M., Allan, J., Canonaco, F., Canagaratna, M., Carbone, S., Crippa, M., Dall Osto, M., Day, D. A., De Carlo, P., Di Marco, C. F., Elbern, H., Eriksson, A., Freney, E., Hao, L., Herrmann, H., Hildebrandt, L., Hillamo, R., Jimenez, J. L., Laaksonen, A., McFiggans, G., Mohr, C., O'Dowd, C., Otjes, R., Ovadnevaite, J., Pandis, S. N., Poulain, L., Schlag, P., Sellegri, K., Swietlicki, E., Tiitta, P., Vermeulen, A., Wahner, A., Worsnop, D., and Wu, H.-C.: Ubiquity of organic nitrates from nighttime chemistry in the European submicron aerosol, Geophys. Res. Lett., 43, 7735–7744, https://doi.org/10.1002/2016gl069239, 2016.

Kodros, J. K., Papanastasiou, D. K., Paglione, M., Masiol, M., Squizzato, S., Florou, K., Skyllakou, K., Kaltsonoudis, C., Nenes, A., and Pandis, S. N.: Rapid dark aging of biomass burning as an overlooked source of oxidized organic aerosol, P. Natl. Acad. Sci. USA, 117, 33028–33033, https://doi.org/10.1073/pnas.2010365117, 2020.

Kodros, J. K., Kaltsonoudis, C., Paglione, M., Florou, K., Jorga, S., Vasilakopoulou, C., Cirtog, M., Cazaunau, M., Picquet-Varrault, B., Nenes, A., and Pandis, S. N.: Secondary aerosol formation during the dark oxidation of residential biomass burning emissions, Environmental Science: Atmospheres, 2, 1221–1236, https://doi.org/10.1039/D2EA00031H, 2022.

Kuang, Y., Zhao, C. S., Tao, J. C., Bian, Y. X., and Ma, N.: Impact of aerosol hygroscopic growth on the direct aerosol radiative effect in summer on North China Plain, Atmos. Environ., 147, 224–233, https://doi.org/10.1016/j.atmosenv.2016.10.013, 2016.

Kuang, Y., He, Y., Xu, W., Yuan, B., Zhang, G., Ma, Z., Wu, C., Wang, C., Wang, S., Zhang, S., Tao, J., Ma, N., Su, H., Cheng, Y., Shao, M., and Sun, Y.: Photochemical Aqueous-Phase Reactions Induce Rapid Daytime Formation of Oxygenated Organic

Aerosol on the North China Plain, Environ. Sci. Technol., 54, 3849–3860, https://doi.org/10.1021/acs.est.9b06836, 2020a.

Kuang, Y., Xu, W., Tao, J., Ma, N., Zhao, C., and Shao, M.: A Review on Laboratory Studies and Field Measurements of Atmospheric Organic Aerosol Hygroscopicity and Its Parameterization Based on Oxidation Levels, Current Pollution Reports, 6, 410–424, https://doi.org/10.1007/s40726-020-00164-2, 2020b.

Kuang, Y., Huang, S., Xue, B., Luo, B., Song, Q., Chen, W., Hu, W., Li, W., Zhao, P., Cai, M., Peng, Y., Qi, J., Li, T., Wang, S., Chen, D., Yue, D., Yuan, B., and Shao, M.: Contrasting effects of secondary organic aerosol formations on organic aerosol hygroscopicity, Atmos. Chem. Phys., 21, 10375–10391, https://doi.org/10.5194/acp-21-10375-2021, 2021.

Kuang, Y., Xu, W., Tao, J., Luo, B., Liu, L., Xu, H., Xu, W., Xue, B., Zhai, M., Liu, P., and Sun, Y.: Divergent Impacts of Biomass Burning and Fossil Fuel Combustion Aerosols on Fog-Cloud Microphysics and Chemistry: Novel Insights From Advanced Aerosol-Fog Sampling, Geophys. Res. Lett., 51, e2023GL107147, https://doi.org/10.1029/2023GL107147, 2024.

Kumar, N. K., Corbin, J. C., Bruns, E. A., Massabò, D., Slowik, J. G., Drinovec, L., Močnik, G., Prati, P., Vlachou, A., Baltensperger, U., Gysel, M., El-Haddad, I., and Prévôt, A. S. H.: Production of particulate brown carbon during atmospheric aging of residential wood-burning emissions, Atmos. Chem. Phys., 18, 17843–17861, https://doi.org/10.5194/acp-18-17843-2018, 2018.

Lareau, N. P. and Clements, C. B.: Environmental controls on pyrocumulus and pyrocumulonimbus initiation and development, Atmos. Chem. Phys., 16, 4005–4022, https://doi.org/10.5194/acp-16-4005-2016, 2016.

Laskin, A., Laskin, J., and Nizkorodov, S. A.: Chemistry of Atmospheric Brown Carbon, Chem. Rev., 115, 4335–4382, https://doi.org/10.1021/cr5006167, 2015.

Li, C., He, Q., Hettiyadura, A. P. S., Käfer, U., Shmul, G., Meidan, D., Zimmermann, R., Brown, S. S., George, C., Laskin, A., and Rudich, Y.: Formation of Secondary Brown Carbon in Biomass Burning Aerosol Proxies through NO$_3$ Radical Reactions, Environ. Sci. Technol., 54, 1395–1405, https://doi.org/10.1021/acs.est.9b05641, 2020a.

Li, M., Wang, X., Lu, C., Li, R., Zhang, J., Dong, S., Yang, L., Xue, L., Chen, J., and Wang, W.: Nitrated phenols and the phenolic precursors in the atmosphere in urban Jinan, China, Sci. Total Environ., 714, 136760, https://doi.org/10.1016/j.scitotenv.2020.136760, 2020b.

Li, Z., Tan, H., Zheng, J., Liu, L., Qin, Y., Wang, N., Li, F., Li, Y., Cai, M., Ma, Y., and Chan, C. K.: Light absorption properties and potential sources of particulate brown carbon in the Pearl River Delta region of China, Atmos. Chem. Phys., 19, 11669–11685, https://doi.org/10.5194/acp-19-11669-2019, 2019.

Lin, P., Bluvshtein, N., Rudich, Y., Nizkorodov, S. A., Laskin, J., and Laskin, A.: Molecular Chemistry of Atmospheric Brown Carbon Inferred from a Nationwide Biomass Burning Event, Environ. Sci. Technol., 51, 11561–11570, https://doi.org/10.1021/acs.est.7b02276, 2017.

Liu, P., Kaplan, J. O., Mickley, L. J., Li, Y., Chellman, N. J., Arienzo, M. M., Kodros, J. K., Pierce, J. R., Sigl, M., Freitag, J., Mulvaney, R., Curran, M. A. J., and McConnell, J. R.: Improved estimates of preindustrial biomass burning reduce the magnitude of aerosol climate forcing in the Southern Hemisphere, Science Advances, 7, eabc1379, https://doi.org/10.1126/sciadv.abc1379, 2021.

Liu, S., Ahlm, L., Day, D. A., Russell, L. M., Zhao, Y., Gentner, D. R., Weber, R. J., Goldstein, A. H., Jaoui, M., Offenberg, J. H., Kleindienst, T. E., Rubitschun, C., Surratt, J. D., Sheesley, R. J., and Scheller, S.: Secondary organic aerosol formation from fossil fuel sources contribute majority of summertime organic mass at Bakersfield, J. Geophys. Res.-Atmos., 117, D00V26, https://doi.org/10.1029/2012JD018170, 2012.

Liu, Y., Wang, T., Fang, X., Deng, Y., Cheng, H., Bacha, A. U., Nabi, I., and Zhang, L.: Brown carbon: An underlying driving force for rapid atmospheric sulfate formation and haze event, Sci. Total Environ., 734, 139415, https://doi.org/10.1016/j.scitotenv.2020.139415, 2020.

Luo, B., Kuang, Y., Huang, S., Song, Q., Hu, W., Li, W., Peng, Y., Chen, D., Yue, D., Yuan, B., and Shao, M.: Parameterizations of size distribution and refractive index of biomass burning organic aerosol with black carbon content, Atmos. Chem. Phys., 22, 12401–12415, https://doi.org/10.5194/acp-22-12401-2022, 2022.

Marufu, L., Dentener, F., Lelieveld, J., Andreae, M. O., and Helas, G.: Photochemistry of the African troposphere: Influence of biomass-burning emissions, J. Geophys. Res.-Atmos., 105, 14513–14530, https://doi.org/10.1029/1999JD901055, 2000.

Mayorga, R. J., Zhao, Z., and Zhang, H.: Formation of secondary organic aerosol from nitrate radical oxidation of phenolic VOCs: Implications for nitration mechanisms and brown carbon formation, Atmos. Environ., 244, 117910, https://doi.org/10.1016/j.atmosenv.2020.117910, 2021.

Odum, J. R., Hoffmann, T., Bowman, F., Collins, D., Flagan, R. C., and Seinfeld, J. H.: Gas/Particle Partitioning and Secondary Organic Aerosol Yields, Environ. Sci. Technol., 30, 2580–2585, https://doi.org/10.1021/es950943+, 1996.

Palm, B. B., Peng, Q., Fredrickson, C. D., Lee, B. H., Garofalo, L. A., Pothier, M. A., Kreidenweis, S. M., Farmer, D. K., Pokhrel, R. P., Shen, Y., Murphy, S. M., Permar, W., Hu, L., Campos, T. L., Hall, S. R., Ullmann, K., Zhang, X., Flocke, F., Fischer, E. V., and Thornton, J. A.: Quantification of organic aerosol and brown carbon evolution in fresh wildfire plumes, P. Natl. Acad. Sci. USA, 117, 29469–29477, https://doi.org/10.1073/pnas.2012218117, 2020.

Petters, M. D., Carrico, C. M., Kreidenweis, S. M., Prenni, A. J., DeMott, P. J., Collett Jr., J. L., and Moosmüller, H.: Cloud condensation nucleation activity of biomass burning aerosol, J. Geophys. Res.-Atmos., 114, D22205, https://doi.org/10.1029/2009JD012353, 2009.

Price, C. L., Preston, T. C., and Davies, J. F.: Hygroscopic Growth, Phase Morphology, and Optical Properties of Model Aqueous Brown Carbon Aerosol, Environ. Sci. Technol., 56, 3941–3951, https://doi.org/10.1021/acs.est.1c07356, 2022.

Qin, Y. M., Tan, H. B., Li, Y. J., Li, Z. J., Schurman, M. I., Liu, L., Wu, C., and Chan, C. K.: Chemical characteristics of brown carbon in atmospheric particles at a suburban site near Guangzhou, China, Atmos. Chem. Phys., 18, 16409–16418, https://doi.org/10.5194/acp-18-16409-2018, 2018.

Rana, M. S. and Guzman, M. I.: Oxidation of Catechols at the Air–Water Interface by Nitrate Radicals, Environ. Sci. Technol., 56, 15437–15448, https://doi.org/10.1021/acs.est.2c05640, 2022.

Rollins, A. W., Browne, E. C., Min, K. E., Pusede, S. E., Wooldridge, P. J., Gentner, D. R., Goldstein, A. H., Liu, S., Day, D. A., Russell, L. M., and Cohen, R. C.: Evidence for NO$_x$ Control over Nighttime SOA Formation, Science, 337, 1210, https://doi.org/10.1126/science.1221520, 2012.

Running, S. W.: Is Global Warming Causing More, Larger Wildfires?, Science, 313, 927, https://doi.org/10.1126/science.1130370, 2006.

Saleh, R.: From Measurements to Models: Toward Accurate Representation of Brown Carbon in Climate Calculations, Current Pollution Reports, 6, 90–104, https://doi.org/10.1007/s40726-020-00139-3, 2020.

Saleh, R., Hennigan, C. J., McMeeking, G. R., Chuang, W. K., Robinson, E. S., Coe, H., Donahue, N. M., and Robinson, A. L.: Absorptivity of brown carbon in fresh and photo-chemically aged biomass-burning emissions, Atmos. Chem. Phys., 13, 7683–7693, https://doi.org/10.5194/acp-13-7683-2013, 2013.

Seinfeld, J. and Pandis, S.: Atmospheric Chemistry and Physics: From Air Pollution to Climate Change, third edn., ISBN 9781119221166, 2016.

Selimovic, V., Yokelson, R. J., McMeeking, G. R., and Coefield, S.: Aerosol Mass and Optical Properties, Smoke Influence on O$_3$, and High NO$_3$ Production Rates in a Western U.S. City Impacted by Wildfires, J. Geophys. Res.-Atmos., 125, e2020JD032791, https://doi.org/10.1029/2020JD032791, 2020.

Song, M., Liu, X., Zhang, Y., Shao, M., Lu, K., Tan, Q., Feng, M., and Qu, Y.: Sources and abatement mechanisms of VOCs in southern China, Atmos. Environ., 201, 28–40, https://doi.org/10.1016/j.atmosenv.2018.12.019, 2019.

Stockwell, C. E., Veres, P. R., Williams, J., and Yokelson, R. J.: Characterization of biomass burning emissions from cooking fires, peat, crop residue, and other fuels with high-resolution proton-transfer-reaction time-of-flight mass spectrometry, Atmos. Chem. Phys., 15, 845–865, https://doi.org/10.5194/acp-15-845-2015, 2015.

Tao, J., Luo, B., Xu, W., Zhao, G., Xu, H., Xue, B., Zhai, M., Xu, W., Zhao, H., Ren, S., Zhou, G., Liu, L., Kuang, Y., and Sun, Y.: Markedly different impacts of primary emissions and secondary aerosol formation on aerosol mixing states revealed by simultaneous measurements of CCNC, H(/V)TDMA, and SP2, Atmos. Chem. Phys., 24, 9131–9154, https://doi.org/10.5194/acp-24-9131-2024, 2024.

Tiitta, P., Leskinen, A., Hao, L., Yli-Pirilä, P., Kortelainen, M., Grigonyte, J., Tissari, J., Lamberg, H., Hartikainen, A., Kuuspalo, K., Kortelainen, A.-M., Virtanen, A., Lehtinen, K. E. J., Komppula, M., Pieber, S., Prévôt, A. S. H., Onasch, T. B., Worsnop, D. R., Czech, H., Zimmermann, R., Jokiniemi, J., and Sippula, O.: Transformation of logwood combustion emissions in a smog chamber: formation of secondary organic aerosol and changes in the primary organic aerosol upon daytime and nighttime aging, Atmos. Chem. Phys., 16, 13251–13269, https://doi.org/10.5194/acp-16-13251-2016, 2016.

Tong, Y., Pospisilova, V., Qi, L., Duan, J., Gu, Y., Kumar, V., Rai, P., Stefenelli, G., Wang, L., Wang, Y., Zhong, H., Baltensperger, U., Cao, J., Huang, R.-J., Prévôt, A. S. H., and Slowik, J. G.: Quantification of solid fuel combustion and aqueous chemistry contributions to secondary organic aerosol during wintertime haze events in Beijing, Atmos. Chem. Phys., 21, 9859–9886, https://doi.org/10.5194/acp-21-9859-2021, 2021.

van der Werf, G. R., Randerson, J. T., Giglio, L., van Leeuwen, T. T., Chen, Y., Rogers, B. M., Mu, M., van Marle, M. J. E., Morton, D. C., Collatz, G. J., Yokelson, R. J., and Kasibhatla, P. S.: Global fire emissions estimates during 1997–2016, Earth Syst. Sci. Data, 9, 697–720, https://doi.org/10.5194/essd-9-697-2017, 2017.

Wang, H., Lu, K., Chen, X., Zhu, Q., Chen, Q., Guo, S., Jiang, M., Li, X., Shang, D., Tan, Z., Wu, Y., Wu, Z., Zou, Q., Zheng, Y., Zeng, L., Zhu, T., Hu, M., and Zhang, Y.: High N$_2$O$_5$ Concentrations Observed in Urban Beijing: Implications of a Large Nitrate Formation Pathway, Environ. Sci. Tech. Let., 4, 416–420, https://doi.org/10.1021/acs.estlett.7b00341, 2017.

Wang, H., Chen, X., Lu, K., Tan, Z., Ma, X., Wu, Z., Li, X., Liu, Y., Shang, D., Wu, Y., Zeng, L., Hu, M., Schmitt, S., Kiendler-Scharr, A., Wahner, A., and Zhang, Y.: Wintertime N$_2$O$_5$ uptake coefficients over the north china plain, Sci. Bull., 65, 765–774, https://doi.org/10.1016/j.scib.2020.02.006, 2020.

Wang, H., Wang, H., Lu, X., Lu, K., Zhang, L., Tham, Y. J., Shi, Z., Aikin, K., Fan, S., Brown, S. S., and Zhang, Y.: Increased night-time oxidation over China despite widespread decrease across the globe, Nat. Geosci., 16, 217–223, https://doi.org/10.1038/s41561-022-01122-x, 2023a.

Wang, J., Nie, W., Cheng, Y., Shen, Y., Chi, X., Wang, J., Huang, X., Xie, Y., Sun, P., Xu, Z., Qi, X., Su, H., and Ding, A.: Light absorption of brown carbon in eastern China based on 3-year multi-wavelength aerosol optical property observations and an improved absorption Ångström exponent segregation method, Atmos. Chem. Phys., 18, 9061–9074, https://doi.org/10.5194/acp-18-9061-2018, 2018a.

Wang, J., Shilling, J. E., Liu, J., Zelenyuk, A., Bell, D. M., Petters, M. D., Thalman, R., Mei, F., Zaveri, R. A., and Zheng, G.: Cloud droplet activation of secondary organic aerosol is mainly controlled by molecular weight, not water solubility, Atmos. Chem. Phys., 19, 941–954, https://doi.org/10.5194/acp-19-941-2019, 2019a.

Wang, J., Ye, J., Zhang, Q., Zhao, J., Wu, Y., Li, J., Liu, D., Li, W., Zhang, Y., Wu, C., Xie, C., Qin, Y., Lei, Y., Huang, X., Guo, J., Liu, P., Fu, P., Li, Y., Lee, H. C., Choi, H., Zhang, J., Liao, H., Chen, M., Sun, Y., Ge, X., Martin, S. T., and Jacob, D. J.: Aqueous production of secondary organic aerosol from fossil-fuel emissions in winter Beijing haze, P. Natl. Acad. Sci. USA, 118, e2022179118, https://doi.org/10.1073/pnas.2022179118, 2021.

Wang, Q., Saturno, J., Chi, X., Walter, D., Lavric, J. V., Moran-Zuloaga, D., Ditas, F., Pöhlker, C., Brito, J., Carbone, S., Artaxo, P., and Andreae, M. O.: Modeling investigation of light-absorbing aerosols in the Amazon Basin during the wet season, Atmos. Chem. Phys., 16, 14775–14794, https://doi.org/10.5194/acp-16-14775-2016, 2016.

Wang, Q., Ye, J., Wang, Y., Zhang, T., Ran, W., Wu, Y., Tian, J., Li, L., Zhou, Y., Hang Ho, S. S., Dang, B., Zhang, Q., Zhang, R., Chen, Y., Zhu, C., and Cao, J.: Wintertime Optical Properties of Primary and Secondary Brown Carbon at a Regional Site in the North China Plain, Environ. Sci. Technol., 53, 12389–12397, https://doi.org/10.1021/acs.est.9b03406, 2019b.

Wang, S.-C., Wang, Y., Estes, M., Lei, R., Talbot, R., Zhu, L., and Hou, P.: Transport of Central American Fire Emissions to the U.S. Gulf Coast: Climatological Pathways and Impacts on Ozone and PM$_{2.5}$, J. Geophys. Res.-Atmos., 123, 8344–8361, https://doi.org/10.1029/2018JD028684, 2018b.

Wang, Y., Hu, M., Wang, Y., Zheng, J., Shang, D., Yang, Y., Liu, Y., Li, X., Tang, R., Zhu, W., Du, Z., Wu, Y., Guo, S., Wu, Z., Lou, S., Hallquist, M., and Yu, J. Z.: The formation of nitro-aromatic compounds under high NO$_x$ and anthropogenic VOC conditions in urban Beijing, China, Atmos. Chem. Phys., 19, 7649–7665, https://doi.org/10.5194/acp-19-7649-2019, 2019c.

Wang, Y., Qiu, T., Zhang, C., Hao, T., Mabato, B. R. G., Zhang, R., Gen, M., Chan, M. N., Huang, D. D., Ge, X., Wang, J., Du, L., Huang, R.-J., Chen, Q., Hoi, K. I., Mok, K. M., Chan, C. K., and Li, Y. J.: Co-photolysis of mixed chromophores affects atmospheric lifetimes of brown carbon, Environmental Science: Atmospheres, 3, 1145–1158, https://doi.org/10.1039/D3EA00073G, 2023b.

Wu, L., Huang, S., Liu, Y., Song, Q., Hu, W., Chen, W., Kuang, Y., Wang, X., Li, W., Peng, Y., Chen, D., Yue, D., Song, W., Yuan, B., Wang, X., and Shao, M.: Source, formation mechanism and inhalation deposition flux of organic aerosols in urban and rural areas of the Pearl River Delta, Acta Scientiae Circumstantiae, 44, 15–28, https://doi.org/10.13671/j.hjkxxb.2023.0194, 2024.

Yang, S., Yuan, B., Peng, Y., Huang, S., Chen, W., Hu, W., Pei, C., Zhou, J., Parrish, D. D., Wang, W., He, X., Cheng, C., Li, X.-B., Yang, X., Song, Y., Wang, H., Qi, J., Wang, B., Wang, C., Wang, C., Wang, Z., Li, T., Zheng, E., Wang, S., Wu, C., Cai, M., Ye, C., Song, W., Cheng, P., Chen, D., Wang, X., Zhang, Z., Wang, X., Zheng, J., and Shao, M.: The formation and mitigation of nitrate pollution: comparison between urban and suburban environments, Atmos. Chem. Phys., 22, 4539–4556, https://doi.org/10.5194/acp-22-4539-2022, 2022.

Yee, L. D., Kautzman, K. E., Loza, C. L., Schilling, K. A., Coggon, M. M., Chhabra, P. S., Chan, M. N., Chan, A. W. H., Hersey, S. P., Crounse, J. D., Wennberg, P. O., Flagan, R. C., and Seinfeld, J. H.: Secondary organic aerosol formation from biomass burning intermediates: phenol and methoxyphenols, Atmos. Chem. Phys., 13, 8019–8043, https://doi.org/10.5194/acp-13-8019-2013, 2013.

Yu, P., Toon, O. B., Bardeen, C. G., Zhu, Y., Rosenlof, K. H., Portmann, R. W., Thornberry, T. D., Gao, R.-S., Davis, S. M., Wolf, E. T., de Gouw, J., Peterson, D. A., Fromm, M. D., and Robock, A.: Black carbon lofts wildfire smoke high into the stratosphere to form a persistent plume, Science, 365, 587, https://doi.org/10.1126/science.aax1748, 2019.

Yu, P., Davis, S. M., Toon, O. B., Portmann, R. W., Bardeen, C. G., Barnes, J. E., Telg, H., Maloney, C., and Rosenlof, K. H.: Persistent Stratospheric Warming Due to 2019–2020 Australian Wildfire Smoke, Geophys. Res. Lett., 48, e2021GL092609, https://doi.org/10.1029/2021GL092609, 2021.

Zhai, M., Kuang, Y., Liu, L., He, Y., Luo, B., Xu, W., Tao, J., Zou, Y., Li, F., Yin, C., Li, C., Xu, H., and Deng, X.: Insights into characteristics and formation mechanisms of secondary organic aerosols in the Guangzhou urban area, Atmos. Chem. Phys., 23, 5119–5133, https://doi.org/10.5194/acp-23-5119-2023, 2023.

Ziemke, J. R., Chandra, S., Duncan, B. N., Schoeberl, M. R., Torres, O., Damon, M. R., and Bhartia, P. K.: Recent biomass burning in the tropics and related changes in tropospheric ozone, Geophys. Res. Lett., 36, L15819, https://doi.org/10.1029/2009GL039303, 2009.